

An algorithm to identify vapor-liquid-liquid equilibria of binary mixtures from vapor-liquid equilibria

Ian H. Bell,^{*,†} Ulrich K. Deiters,[‡] and Andreas Jäger[¶]

[†]*Applied Chemicals and Materials Division, National Institute of Standards and Technology, Boulder, CO 80305*

[‡]*Institute of Physical Chemistry, University of Cologne, 50939 Köln, Germany*

[¶]*Institute of Power Engineering, Faculty of Mechanical Science and Engineering, Technische Universität Dresden, Helmholtzstraße 14, 01069 Dresden, Germany*

E-mail: ian.bell@nist.gov

Abstract

In this work we demonstrate that tracing the vapor-liquid equilibria for binary mixtures also includes all the information needed to obtain the three-phase-line if one is present. This simple observation serves as a launching point for calculation of liquid-liquid equilibrium and three-phase equilibria, even when one component is supercritical. We close with the demonstration of the automatic construction of an isothermal pressure-composition figure, a capability enabled by solving for the three-phase state. Examples in the Python programming language demonstrate in detail how the method is applied.

1 Introduction

The calculation of multi-phase equilibria from a thermodynamic model appears at first glance to be a straightforward task. One must “simply” equate the chemical potentials of all components in all phases and the pressures in all phases. *Et voilà!* On the contrary, reliable calculations for phase equilibria are by no means guaranteed, and as the model becomes increasingly mathematically involved (often positively correlated with its accuracy), the likelihood of

trouble increases. See for instance the criticality plots in Ref. 1 for one example how a more complicated (and accurate) model can cause challenges in calculating critical points. Therefore, it is desirable to develop algorithms that are extremely reliable, even if they might incur a computational speed penalty (though this penalty is by no means guaranteed). For this reason the authors have been developing routines²⁻⁶ for phase equilibria that have at their core the notion of starting at a well-characterized point (a pure component value for instance), and then tracing along the phase equilibria surface from there, rather than carrying out a “blind” phase equilibrium calculation for which the algorithm must have a good (sometimes *very* good) estimate of phase densities and compositions in order to converge to the correct phase equilibrium solution.

The three-phase (vapor, liquid, liquid) solution obtained from the two-phase vapor-liquid equilibria is a good launching point for liquid-liquid equilibria calculations. Therefore, the focus of this paper is on how to obtain this three-phase equilibrium in a very reliable fashion. The algorithm we propose can be concisely expressed, and implemented with the use of existing computational tools. A key advantage of the approach proposed here is that because of

the use of tracing we never solve for density at a given temperature, pressure and composition, a task that is challenging for some thermodynamic models,^{7,8} and is not entirely foolproof for cubic equations of state either.⁹

While the construction of isothermal pressure-composition diagrams including three-phase curves is not novel (a few examples: Refs. 6,10–15), the literature is quiet on the details of the process. Some authors proposed algorithms for constructing isothermal pressure-composition diagrams for rather special applications, as for example the precipitation of asphaltene phases¹⁶ or multi-phase equilibria including minerals in geosciences.¹⁷ Michelsen and Mollerup¹⁸ (page 310-317) propose two different methods for identifying three-phase vapor-liquid-liquid equilibria (VLLE) when constructing p-x or T-x diagrams. The first method is tracing the vapor-liquid equilibrium (VLE) to meta- and unstable conditions. In the case that the binary mixture exhibits a three-phase equilibrium, there will be a minimum and a maximum in the bubble line, which can be detected by the algorithm. Michelsen and Mollerup¹⁸ suggest to subsequently identify the same vapor phase which is in equilibrium with two different liquids in order to determine the three-phase equilibrium. The second method suggested by Michelsen and Mollerup¹⁸ is a sophisticated method for finding the VLLE by first generating a guess value for pressure (in case of an isotherm in a p-x diagram). They state that the guess value for pressure is in most cases overestimated. Therefore, most likely, a liquid-liquid equilibrium (LLE) will be found and subsequently the LLE is traced to lower pressures until the VLLE can be determined. Venkatarathnam¹⁴ proposed a density marching method to construct p-x and T-x diagrams including the vapor-liquid-liquid equilibrium line. The algorithm can pass through meta- and unstable VLE and LLE solutions. From the intersection of the stable liquid and the stable vapor branch, the VLLE can be located. Alternatively, Venkatarathnam¹⁴ proposes to find the VLLE before constructing the diagram, similar to the approach discussed in Ref. 18. For this case, Venkatarathnam¹⁴ suggests to do

a three-phase bubble point calculation, see Ref. 19. Venkatarathnam¹⁴ states that the proposed algorithm might fail in some special cases. Other publications propose algorithms for the three-phase flash problem^{20–24} or methods for tracing the vapor-liquid-liquid equilibrium lines given a suitable starting point.²⁵ Based on their previous work,²⁵ Cismondi and Michelsen²⁶ proposed a method to construct p-x and T-x diagrams by first calculating critical points and three-phase lines and then subsequently constructing all two phase regions. Many of the algorithms proposed in the literature employ the tangent plane distance criterion^{27,28} in order to test for phase stability. In the thermophysical property software TREND,²⁹ three-phase equilibria of binary mixtures can currently only be automatically calculated when choosing pressure and enthalpy or pressure and entropy as input. The corresponding algorithms implemented in TREND are described in Ref. 22.

The REFPROP software library is the industry standard for high-accuracy thermophysical property models and explicitly does not include the consideration of multiphase equilibria. The warning message when opening the REFPROP user interface for the first time reads: “The present version is limited to vapor-liquid equilibrium (VLE) only and does not address liquid-liquid equilibrium (LLE), vapor-liquid-liquid equilibrium (VLLE) or other complex forms of phase equilibrium.” The work in this paper begins the process of making REFPROP able to solve for multi-phase equilibria.

Therefore, in this work we propose a reproducible and robust approach for calculating three-phase equilibria by using the concept of isochoric thermodynamics,^{2–6} which can also be used to automatically construct p-x diagrams for binary mixtures.

2 Algorithm

Before getting into the details, the approach is explained in words:

- Vapor-liquid-liquid equilibrium (VLLE) is the connection of two conventional vapor-liquid-equilibrium (VLE) solutions.

So to obtain the VLLE solution, find the two VLE solutions with the same vapor phase and different liquid phases.

- In order to obtain this VLLE solution, first we look for vapor phase intersections of the vapor-liquid phase equilibria in pressure-composition coordinates along an isotherm. There should be one valid intersection if VLLE is present.
- If the vapor phases obtained are close to being identical, then VLLE has likely been found. Polishing of the approximate solution from intersection yields the equilibrium state for the three phases.

2.1 Isochoric Thermodynamics

In the formalism of isochoric thermodynamics, the Helmholtz energy density Ψ is the independent variable and the dependent variables are temperature T and the vector of molar concentrations of the components $\boldsymbol{\rho}$

$$\Psi(T, \boldsymbol{\rho}) = a(T, \boldsymbol{\rho}) \times \rho \quad (1)$$

and all derivatives are obtained from derivatives of this potential with respect to temperature and molar concentrations. The molar Helmholtz energy a is obtained from the thermodynamic model (which may be considered to be arbitrary at this point). Conversion to the more commonly used molar density and mole fractions go like

$$\rho = \sum_i \rho_i \quad (2)$$

$$x_i = \frac{\rho_i}{\rho} \quad (3)$$

The derivatives *along* the phase equilibrium surface along an isotherm can be defined analytically in terms of the Helmholtz energy density. A very similar process applies for derivatives taken along isobars or isopleths (curves of constant mixture composition). For a binary mixture, the derivatives of each phase are obtained from sequentially solving two linear problems

for the isothermal case:⁵

$$\begin{bmatrix} (\mathbf{H}' \boldsymbol{\rho}'')^\top \\ (\mathbf{H}' \boldsymbol{\rho}')^\top \end{bmatrix} \frac{d\boldsymbol{\rho}'}{dp} \Big|_{T,\sigma} = \begin{bmatrix} 1 \\ 1 \end{bmatrix} \quad (4)$$

$$\mathbf{H}'' \frac{d\boldsymbol{\rho}''}{dp} \Big|_{T,\sigma} = \mathbf{H}' \frac{d\boldsymbol{\rho}'}{dp} \Big|_{T,\sigma} \quad (5)$$

where the bracketed term in the left-hand-side of Eq. (4) has dimensions of 2×2 and the $\boldsymbol{\rho}$ are considered to be column vectors. The matrix \mathbf{H} is the Hessian of the Helmholtz energy density with entries given by

$$H_{ij} = \begin{cases} \frac{1}{\rho_i} + \left(\frac{\partial^2 \Psi^r}{\partial \rho_i^2} \right)_{\rho_{k \neq i}} & \text{if } i = j \\ \left(\frac{\partial^2 \Psi^r}{\partial \rho_i \partial \rho_j} \right) & \text{if } i \neq j \end{cases} \quad (6)$$

Deriving a set of differential equations along the phase equilibrium surface is the first step. The next step is to develop an algorithm for integrating the set of differential equations along the phase envelope. In principle it is possible to integrate these equations with temperature, pressure, or a molar concentration of a component as the tracing variable,³⁻⁵ but it is difficult to know *a priori* which tracing approach is most appropriate for a particular case (curve of constant temperature, pressure, or molar composition), and not all will be able to yield a complete trace due to local extrema in the tracing variable curve.⁶ A new approach eliminating the need to select the tracing variable is to trace in terms of an arclength variable. This parametric tracing approach does not require any user intervention to trace the isoline or selection of tracing variable. The arclength parameter (the *parameter* in parametric tracing) is not a measurable quantity, rather it is a mathematical convenience. But this approach has proven its reliability in tracing complex phase equilibria behaviors as well as tracing critical curves by a similar approach.³⁰

The differential of the new parametric tracing variable t is defined based on the norm of the differentials of the concentration vectors:

$$dt = \pm \sqrt{(d\boldsymbol{\rho}')^2 + (d\boldsymbol{\rho}'')^2} \quad (7)$$

where the sign of the \pm is selected such that the tracing does not result in an abrupt change in direction; phase envelopes tend to be smooth. The sign may need to be updated during the course of integration, and needs to be specified at the beginning of the integration. The norm operation is defined by

$$(d\rho^x)^2 = \sum_i (d\rho_i^x)^2, \chi = ', '' \quad (8)$$

and dividing through by the differential of p yields the derivative at constant temperature

$$\frac{dt}{dp} = \pm \sqrt{\left(\left.\frac{d\rho'}{dp}\right|_{T,\sigma}\right)^2 + \left(\left.\frac{d\rho''}{dp}\right|_{T,\sigma}\right)^2} \quad (9)$$

from which derivatives of the concentration vectors may be defined⁶

$$\frac{d\rho'}{dt} = \left.\frac{d\rho'}{dp}\right|_{T,\sigma} \frac{dp}{dt} \quad (10)$$

$$\frac{d\rho''}{dt} = \left.\frac{d\rho''}{dp}\right|_{T,\sigma} \frac{dp}{dt} \quad (11)$$

and the pressure derivatives are as given above in Eq. (4) and Eq. (5).

The integration of the above set of differential equations, for which an adaptive step size algorithm should be used, traces away from a known state. In this work, we always start our tracing from a pure fluid endpoint. That is, we carry out a pure fluid phase equilibrium calculation and the values for the co-existing densities for a given temperature are obtained. From this pure fluid solution is obtained the values of ρ at a pure fluid endpoint. Supposing the pure-fluid saturated liquid and vapor densities of component A are ρ'_A and ρ''_A , respectively, the vector of molar densities would be $\rho' = [\rho'_A, 0]$ for the liquid phase $\rho'' = [\rho''_A, 0]$ for the vapor phase for the mixture of A + B. If the temperature is subcritical for both members of the binary mixture, the tracing can in principle be initiated at either pure fluid endpoint. There are some additional numerical concerns in the case of infinite dilution (one component density being zero), which are handled properly in the code, and described in the literature.³

Tracing proceeds until a) the other pure fluid has been obtained (a mole fraction less than zero is obtained) or b) when a critical point is approached. Heuristic metrics in the tracer are used to stop when either of these cases are encountered, as well as to handle some other corner cases (not relevant to the system of nitrogen + ethane, which we will be using as an example). An advantage of this approach is that azeotropy is not a hindrance to the tracing.

2.2 Obtaining Approximate Solution

The advent of parametric tracing of phase equilibria⁶ has resulted in a very reliable means of obtaining contiguous portions of cross-sections of the phase-equilibrium surface. In this case, we use the Python package `isochoric` to do the tracing, and the results for a low-temperature isotherm of 120.3420 K for the mixture of nitrogen + ethane are presented in Figure 1. To generate this figure, one trace was initiated at pure nitrogen ($x_1 = 1$ at a pressure of 2.55 MPa) and another at pure ethane ($x_1 = 0$ at a pressure of 370 Pa). Each portion of the isothermal phase equilibria was traced with the parametric tracer until it terminated, yielding the curves shown in the figure. Note that the right portion of the graph has a very different axis scale to improve the legibility. The calculated values are given in the tables in the supporting information for verification purposes.

In this figure, the three-phase pressure is highlighted, and the liquid-phase solutions are rendered more subtly so that the focus is on the vapor phase. The intersection of the vapor phase solutions occurs at the three-phase solution. The thermodynamic state can be fully specified by the temperature, pressure and composition. The crossing of the vapor phase curves (crossing indicating that they are at the same composition and pressure) implies that the thermodynamic states must be identical.

While it is by no means guaranteed, in this case the three-phase solution is in very good agreement with experimental data from the literature because the thermodynamic model represents the experimental data well. The

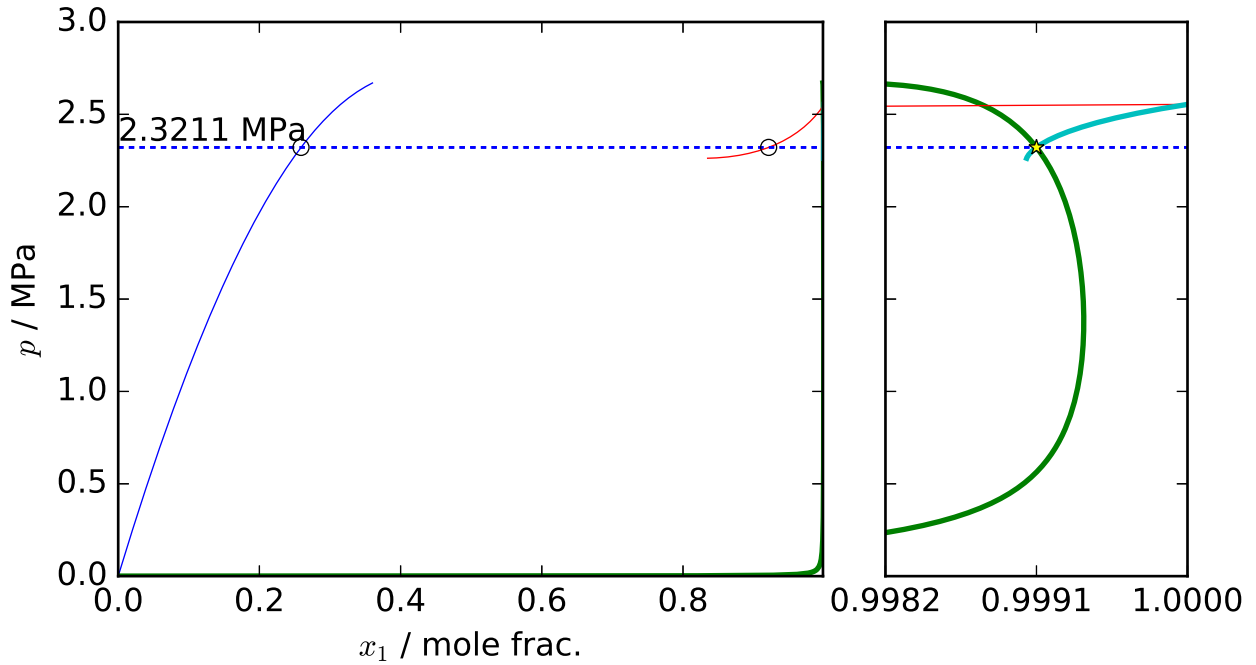


Figure 1: Nitrogen(1) + ethane(2) tracing at a temperature of 120.3420 K. Open markers are experimental values from Llave et al.³¹ Thick lines are vapor phases, thin lines are liquid phases.

isotherm temperature was selected because it matches a temperature measured by Llave et al.³¹ (after conversion to the ITS-90 temperature scale³²) and is below the critical temperature for both fluids.

In this particular case, a single trace, started at either of the pure components, marching in ρ_1 , would have also allowed for the full trace in one shot, but that is not guaranteed, and the parametric approach is more generally applicable. The advantage of the parametric approach is that no control variables or human decisions are needed; the algorithm stops when it hits a critical point or a pure fluid.

While the human vision system is an advanced tool for identifying intersections of space curves in two dimensions, computers struggle with this task. Curve intersection algorithms tend to be surprisingly slow, and there are many numerical pitfalls that can be introduced (degeneracy, etc.). Vectorization allows for a more computationally efficient solution, as is necessary here. The intersection problem is delegated to specialized routines, providing the arrays of points x_A, y_A in the search for self-intersection of space curve A, or x_A, y_A, x_B, y_B for the case of intersection of the space curves A

and B. Figure 2 shows the case of a Maclaurin trisectrix intersecting itself and intersecting a line. The mathematically continuous curves are discretized, to highlight the fact that the same discretized approach is needed in this work. These two cases are identical to the self- and cross-intersections needed in this work.

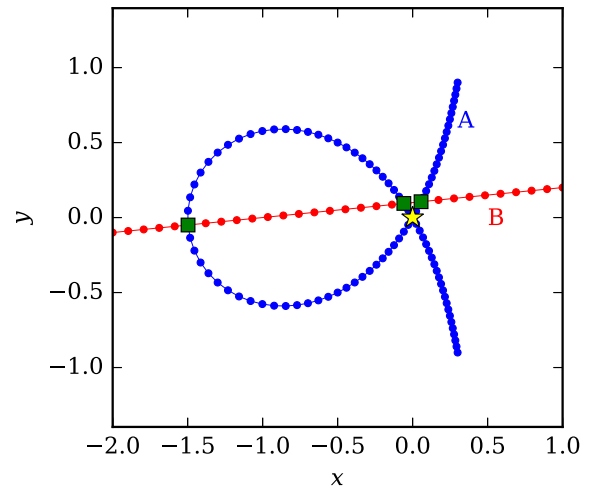


Figure 2: The Maclaurin trisectrix (curve A), given by $x = a(t^2 - 3)/(t^2 + 1)$, $y = at(t^2 - 3)/(t^2 + 1)$, with t in $[-3, 3]$ and $a = 0.5$, intersecting itself (star) and intersecting the curve B given by the line $y = 0.1x + 0.1$ (squares)

The intersection routines return the indices of the array where the intersection occurred and linearly interpolated values of x and y at the intersection. Returned intersections then are filtered to remove undesirable solutions caused by numerical artifacts, mostly in the self-intersection case, where spurious self-intersection is much more likely, especially around critical points and cusps. The filter is that the two endpoints of each of the line segments forming the intersection should be thermodynamically stable, which is guaranteed by $\lambda_1(\mathbf{H}) > 0.01$ (λ_1 being the minimum eigenvalue of the Hessian matrix \mathbf{H} defined by Eq. (6)).

Locating the vapor phase intersection yields the pressure of the three-phase solution and the composition of the vapor phase. The next step is to backwards interpolate the liquid-phase portions of the trace(s) to obtain the approximate molar concentrations for the liquid phases. To do so, each of the space curves $\rho'_k(p)$ is linearly interpolated for the three-phase pressure obtained from intersection to yield the estimated values at VLLE. This yields the molar concentrations of each component in the liquid phases that are in equilibrium with the paired vapor phase solution. While not especially accurate in general, the error introduced by linear interpolation a) is very small because the curves are nearly linear near the intersections b) will be removed by the phase equilibrium polishing routine described next. A numerical example of the procedure is provided below.

2.3 Polishing

Once an approximate three-phase solution defined by the molar concentration arrays in each phase (ρ' , ρ'' , ρ''') has been identified for a given temperature, the next step is to polish the solution to obtain the “true” thermodynamic solution to numerical precision. The phase equilibrium problem is expressed as

$$\mu'_k = \mu''_k = \mu'''_k \quad (12)$$

$$p' = p'' = p''' \quad (13)$$

for each of the k components (here $k = 2$ because there are two components) in the three (','',''') phases. For a binary mixture at fixed temperature there are six independent variables (two molar concentrations per phase), and the six equations to be forced to zero by a non-linear rootfinding algorithm are:

$$\mathbf{r} = \begin{bmatrix} p' - p'' \\ p'' - p''' \\ \mu'_0 - \mu''_0 \\ \mu'_0 - \mu'''_0 \\ \mu'_1 - \mu''_1 \\ \mu'_1 - \mu'''_1 \end{bmatrix} \quad (14)$$

Dropping portions of the chemical potential that are the same in each phase, the phase equilibrium problem can be refactored⁵ in terms of residual properties only as

$$\Omega_k^r = \frac{1}{RT} \left(\frac{\partial \Psi^r}{\partial \rho_k} \right)_{\rho_{j \neq k}, T} + \ln(\rho_k) \quad (15)$$

yielding

$$\mathbf{r} = \begin{bmatrix} p' - p'' \\ p'' - p''' \\ (\Omega^r)'_0 - (\Omega^r)''_0 \\ (\Omega^r)'_0 - (\Omega^r)'''_0 \\ (\Omega^r)'_1 - (\Omega^r)''_1 \\ (\Omega^r)'_1 - (\Omega^r)'''_1 \end{bmatrix} \quad (16)$$

The residua of chemical potentials could also be expressed as differences in fugacities with no loss in generality. The derivation is in Section 2 of the supporting information.

In this case, we know that the guess value for the three-phase solution is very close to the full solution, so standard multidimensional rootfinding can be used. In this case we used the `root` function from the `scipy.optimize` package which uses finite differentiation to build the Jacobian matrix. If additional speed were needed for this rootfinding step, analytical derivatives of the residual functions could be derived.

2.4 Supercritical Extension

If the mixture is supercritical (is above the critical temperature of at least one component), it is no longer possible to initialize a trace from at least one of the pure fluids at its saturation temperature because the pure fluid solution does not exist. An alternative approach is therefore needed, following the approach used for the other phase equilibrium tracing: we express the conditions of three-phase equilibrium algebraically, take the differentials of these conditions, and develop systems of differential equations along the phase envelope. We then integrate this system of differential equations from a subcritical temperature where the three-phase solution can be obtained (with the molar concentrations ρ' , ρ'' , and ρ''') in order to obtain supercritical solutions. More precisely, we obtain a set of derivatives $d\rho^\alpha/dT$ for α corresponding to each of the three phases, and integrate this system of derivatives from a subcritical temperature to the supercritical temperature of interest to obtain the molar concentrations in each phase. If temperature and molar concentrations are known in each phase, so too is the pressure from $p = f(T, \rho)$; the pressure should be the same in each phase. The mathematics required for these derivatives are summarized in Fig. 3 and laid out in detail in Section 1 of the supporting information.

3 Results

In order to demonstrate the approach, we have selected the mixture nitrogen + ethane. This non-polar and non-associating system has been considered because three independent experimental datasets from the literature exist for cross-comparison. In this work we use the multi-fluid approach with the pure fluid EOS from their respective reference equation of state (nitrogen: Ref. 33, ethane: Ref. 34) and the mixture model from GERG-2004.³⁵ This is the default model used in REFPROP,³⁶ CoolProp,³⁷ and TREND.²⁹ This system can also be reasonably modeled by a range of other less accurate thermodynamic models (cubic EOS, etc.). The approach employed in this work is

agnostic as to the particular equation of state selected; all that is needed is an implementation of α^r and its thermodynamic derivatives.

The entire codebase of the tracer is available at <https://github.com/usnistgov/isochoric>, which is available in the python package index (PYPI). Version 0.10.2 of the tracer was used to generate all the figures in this paper. The scripts used to generate the figures in the paper as well as an environment file for conda are included in the deposited data at <https://doi.org/10.18434/mds2-2487>. The thermodynamic backend is the core thermodynamic backend of CoolProp.³⁷

In order to explain the procedure in somewhat more detail, a worked example is provided here along with plenty of significant digits to ensure that the values are in agreement. Again we select the 120.3420 K isotherm, matching the data from Llave et al.,³¹ which has the two traces shown in Fig. 1. The numerical intersection code yields the approximate solutions for the molar concentrations of the three phases (in units of mol/m³, for the pair nitrogen + ethane in that order) of

$$\rho' = [5676.16238, 16112.5673] \quad (20)$$

$$\rho'' = [19895.8089, 1659.22076] \quad (21)$$

$$\rho''' = [3686.40274, 3.27912599] \quad (22)$$

for which the calculated values of pressure (in Pa) in the three phases are

$$p^{','','''} = [2328534, 2323538, 2326234] \quad (23)$$

After carrying out the complete phase equilibrium, the pressures are equated to numerical precision, and the molar concentrations of each of the phases (in units of mol/m³, with the same ordering as before) are equal to

$$\rho' = [5640.76015, 16141.2539] \quad (24)$$

$$\rho'' = [19890.1584, 1698.9167] \quad (25)$$

$$\rho''' = [3669.84793, 3.25894533] \quad (26)$$

Comparing these results with the approximate solution above highlights that the pol-

$$\begin{bmatrix} (\Psi'(\boldsymbol{\rho}'' - \boldsymbol{\rho}'))^\top \\ (\Psi'(\boldsymbol{\rho}''' - \boldsymbol{\rho}'))^\top \end{bmatrix} \cdot \frac{d\boldsymbol{\rho}'}{dT} = \begin{bmatrix} \left[\left(\frac{\partial \boldsymbol{\mu}''}{\partial T} \right)_\rho - \left(\frac{\partial \boldsymbol{\mu}'}{\partial T} \right)_\rho \right] \cdot \boldsymbol{\rho}'' - \left[\left(\frac{\partial p''}{\partial T} \right)_\rho - \left(\frac{\partial p'}{\partial T} \right)_\rho \right] \\ \left[\left(\frac{\partial \boldsymbol{\mu}'''}{\partial T} \right)_\rho - \left(\frac{\partial \boldsymbol{\mu}'}{\partial T} \right)_\rho \right] \cdot \boldsymbol{\rho}''' - \left[\left(\frac{\partial p'''}{\partial T} \right)_\rho - \left(\frac{\partial p'}{\partial T} \right)_\rho \right] \end{bmatrix} \quad (17)$$

$$\Psi'' \frac{d\boldsymbol{\rho}''}{dT} = \Psi' \frac{d\boldsymbol{\rho}'}{dT} - \left[\left(\frac{\partial \boldsymbol{\mu}''}{\partial T} \right)_\rho - \left(\frac{\partial \boldsymbol{\mu}'}{\partial T} \right)_\rho \right] \quad (18)$$

$$\Psi''' \frac{d\boldsymbol{\rho}'''}{dT} = \Psi' \frac{d\boldsymbol{\rho}'}{dT} - \left[\left(\frac{\partial \boldsymbol{\mu}'''}{\partial T} \right)_\rho - \left(\frac{\partial \boldsymbol{\mu}'}{\partial T} \right)_\rho \right] \quad (19)$$

Figure 3: The set of equations to be sequentially solved in order to obtain the temperature derivatives $d\boldsymbol{\rho}'/dT$, $d\boldsymbol{\rho}''/dT$, and $d\boldsymbol{\rho}'''/dT$ along the VLLE curve. In the first equation, the bracketed term in the left-hand-side is of dimension 2×2 and $\boldsymbol{\mu}$ and $\boldsymbol{\rho}$ are considered to be column vectors.

ishing is doing only a tiny modification to the phase equilibrium solution because the tracing + intersection approach tracks so closely the true thermodynamic solution.

To begin, we consider the three-phase pressure, as shown in Fig. 4. The critical temperature of nitrogen, at 126.192 K, is the lower of the two pure components, so for any temperatures above 126 K, a full phase equilibrium solution was carried out at 120 K (low enough to avoid numerical difficulties too close to the critical point of nitrogen) and then the system of differential equations shown in Fig. 3 was integrated from 120 K to the temperature of interest, yielding an approximate (but very good) VLLE solution at the temperature of interest. A complete phase equilibrium solution was then carried out at the target temperature to obtain the exact solution. We plot the obtained VLLE pressure according to the literature sources^{31,38,39} and the model values as a function of temperature, as well as the relative deviations. Aside from the data of Yu et al.,³⁸ which we deem to be less reliable, the relative deviations in pressure are all within 4%, with a clear systematic bias of approximately -3%.

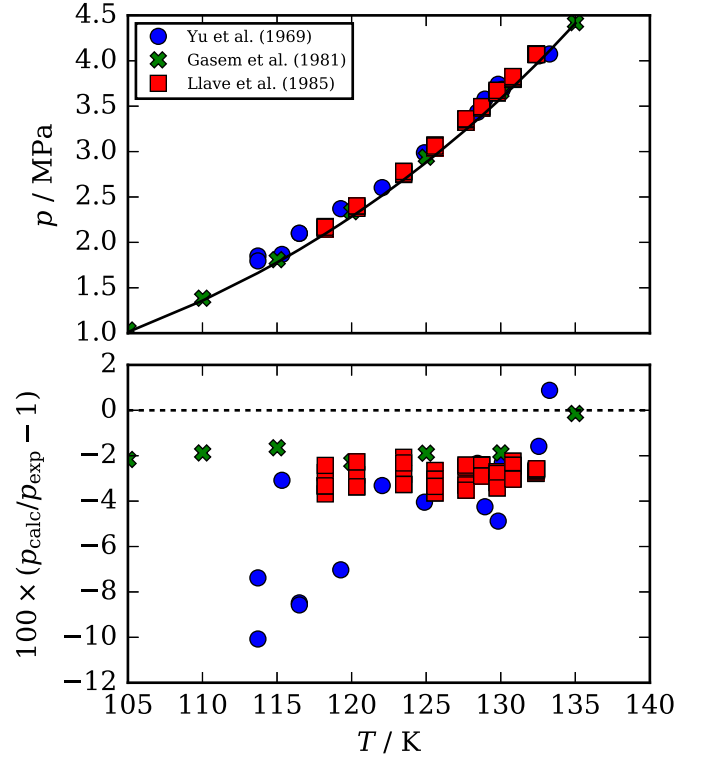


Figure 4: Three phase pressure and deviations as a function of temperature for nitrogen + ethane.

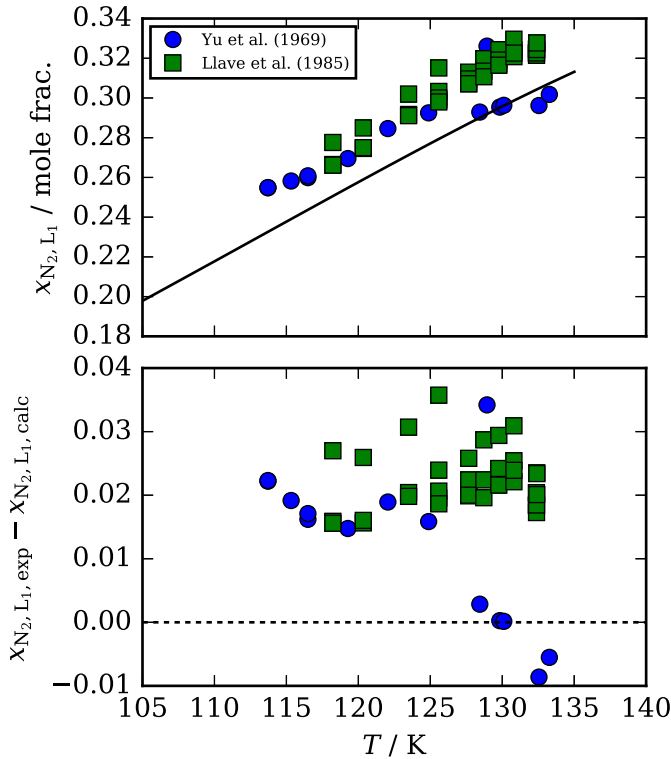


Figure 5: Three phase mole fraction of nitrogen in the nitrogen-weak liquid phase L_1 and model deviations as a function of temperature for nitrogen + ethane.

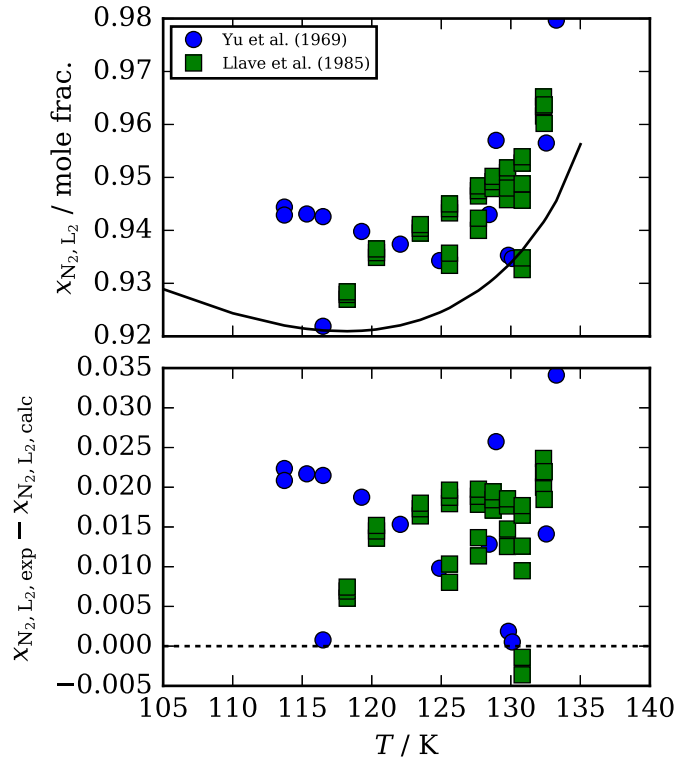


Figure 6: Three phase mole fraction of nitrogen in the nitrogen-rich liquid phase L_2 and model deviations as a function of temperature for nitrogen + ethane.

On the other hand, the liquid phase compositions are less well predicted. Figure 5 and Fig. 6 show the same figure for the mole fractions of nitrogen in each liquid phase. While the qualitative agreement is good, the quantitative agreement is poor. The disagreement is due to the thermodynamic model itself, not a problem in the three-phase solving routines.

3.1 Automatic p-x Diagrams

A challenge when trying to automatically construct isothermal pressure-composition diagrams for binary mixtures is that portions of the phase equilibrium not attached to the pure fluid are difficult to obtain. For instance, in the case of nitrogen + ethane, at a temperature of 130 K, it is not possible to initialize the tracing at pure nitrogen because we are above the critical point of nitrogen. On the other hand, if the three-phase curve has been obtained from a calculation at lower temperature followed by integration to higher temperature,

it is possible to initiate the three portions of the p - x phase boundary from the three solutions: L_1+L_2 , $V+L_1$, and $V+L_2$. In this way we can automatically build some p - x boundaries that are difficult to construct by other means. As a demonstration, taking inspiration from a similar figure for nitrogen + ethylene in Gasem et al.,³⁹ we present in Fig. 7 the pressure-composition diagram for nitrogen + ethane at 130 K. First the three-phase solution is obtained as described above, yielding the L_1 , L_2 , and V equilibrium phases. Then parametric tracing is launched away from the three-phase solution, yielding the p - x plot of the isotherm. This approach is identical to that used in Fig. 8 of Ref. 6. The computational code is quite efficient; the entire diagram is plotted in less than a second.

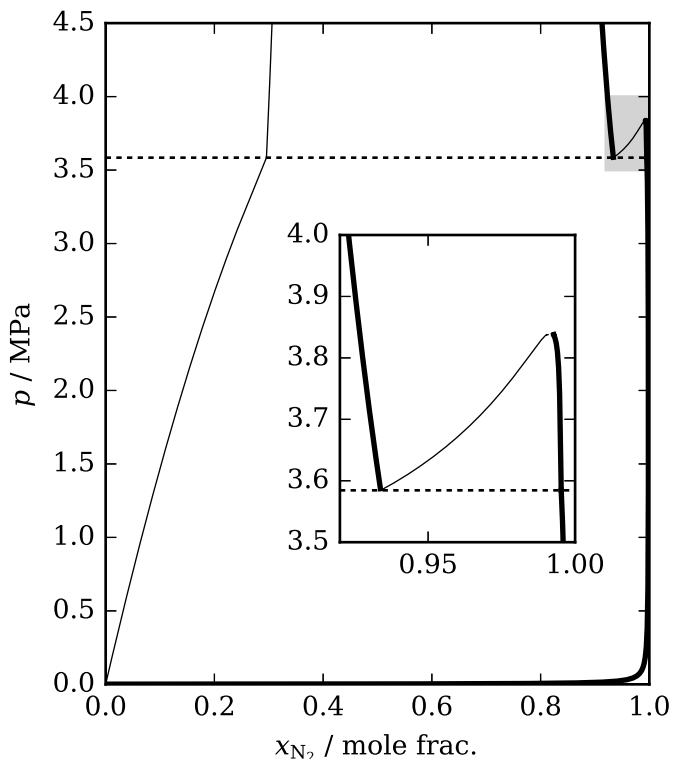


Figure 7: Pressure-composition plot for nitrogen + ethane at 130 K constructed by obtaining the three-phase solution and parametrically tracing away from the three-phase solution. “Vapor” phases are thick curves (the other liquid phase for LLE portion), and “liquid” phases are thin curves. The inset is in the same units as the main figure, and is indicated by the shaded region.

Conclusions

This method is able to find the three-phase solution if it exists, in a reliable fashion. Only very minimal assistance from the user is needed to guide the algorithm, and this guidance is only needed when the temperature is outside the range of allowed saturation temperatures of the two pure component EOS.

There is nothing special about constructing a constant temperature cross-section of the phase equilibrium surface; constant pressure cross-sections could also be constructed, following the same procedure for parametric tracing, followed by curve intersection, and obtaining the VLLE solution.

4 Data Availability

The scripts and data used to generate the figures in this paper have been deposited in the NIST institutional repository at <https://doi.org/10.18434/mds2-2487>

5 Supplementary Material

The supplementary material includes the derivation of the three-phase temperature derivatives

Acknowledgments

The authors thank Ivan Antolovic from TU Berlin for provoking us to revisit this topic, and Stefan Herrig for bringing this problem to our attention in the first place.

References

- (1) Bell, I. H.; Jäger, A. Calculation of critical points from Helmholtz-energy-explicit mixture models. *Fluid Phase Equilib.* **2017**, *433*, 159–173, DOI: 10.1016/j.fluid.2016.10.030.
- (2) Deiters, U. K.; Kraska, T. In *High-Pressure Fluid Phase Equilibria: Phe-*

- nomenclology and Computation*; Kiran, E., Ed.; Elsevier, 2012.
- (3) Deiters, U. K. Differential equations for the calculation of fluid phase equilibria. *Fluid Phase Equilib.* **2016**, *428*, 164–173, DOI: 10.1016/j.fluid.2016.04.014.
 - (4) Deiters, U. K. Differential equations for the calculation of isopleths of multicomponent fluid mixtures. *Fluid Phase Equilib.* **2017**, *447*, 72–83, DOI: 10.1016/j.fluid.2017.03.022.
 - (5) Bell, I. H.; Deiters, U. K. On the construction of binary mixture p - x and T - x diagrams from isochoric thermodynamics. *AIChE J.* **2018**, *64*, 2745–2757, DOI: 10.1002/aic.16074.
 - (6) Deiters, U. K.; Bell, I. H. Calculation of phase envelopes of fluid mixtures through parametric marching. *AIChE J.* **2019**, *65*, e16730, DOI: 10.1002/aic.16730.
 - (7) Gernert, J.; Jäger, A.; Span, R. Calculation of phase equilibria for multicomponent mixtures using highly accurate Helmholtz energy equations of state. *Fluid Phase Equilib.* **2014**, *375*, 209–218, DOI: 10.1016/j.fluid.2014.05.012.
 - (8) Bell, I. H.; Alpert, B. K. Exceptionally reliable density-solving algorithms for multiparameter mixture models from Chebyshev expansion rootfinding. *Fluid Phase Equilib.* **2018**, *476B*, 89–102, DOI: 10.1016/j.fluid.2018.04.026.
 - (9) Bell, I. H.; Deiters, U. K. Superancillary Equations for Cubic Equations of State. *Ind. Eng. Chem. Res.* **2021**, *60*, 9983–9991, DOI: 10.1021/acs.iecr.1c00847.
 - (10) Privat, R.; Jaubert, J.-N. Classification of global fluid-phase equilibrium behaviors in binary systems. *Chem. Eng. Res. Des.* **2013**, *91*, 1807–1839, DOI: 10.1016/j.cherd.2013.06.026.
 - (11) Gernert, J.; Span, R. EOS-CG: A Helmholtz energy mixture model for humid gases and CCS mixtures. *J. Chem. Thermodyn.* **2016**, *93*, 274–293, DOI: 10.1016/j.jct.2015.05.015.
 - (12) Aasen, A.; Hammer, M.; Müller, E. A.; Wilhelmsen, Ø. Equation of state and force fields for Feynman-Hibbs-corrected Mie fluids. II. Application to mixtures of helium, neon, hydrogen, and deuterium. *J. Chem. Phys.* **2020**, *152*, 074507, DOI: 10.1063/1.5136079.
 - (13) Aasen, A.; Hammer, M.; Lasala, S.; Jaubert, J.-N.; Wilhelmsen, Ø. Accurate quantum-corrected cubic equations of state for helium, neon, hydrogen, deuterium and their mixtures. *Fluid Phase Equilibria* **2020**, *524*, 112790, DOI: 10.1016/j.fluid.2020.112790.
 - (14) Venkatarathnam, G. Density Marching Method for Drawing Phase Envelopes. 3. P-xy Diagrams of Binary Mixtures. *Ind. Eng. Chem. Res.* **2017**, *56*, 13894–13904, DOI: 10.1021/acs.iecr.7b03188.
 - (15) Qian, J.-W.; Privat, R.; Jaubert, J.-N.; Coquelet, C.; Ramjugernath, D. Fluid-phase-equilibrium prediction of fluorocompound-containing binary systems with the predictive E-PPR78 model. *Int. J. Refrig.* **2017**, *73*, 65–90, DOI: 10.1016/j.ijrefrig.2016.09.013.
 - (16) Agger, C. S.; Sørensen, H. Algorithm for Constructing Complete Asphaltene PT and Px Phase Diagrams. *Ind. Eng. Chem. Res.* **2017**, *57*, 392–400, DOI: 10.1021/acs.iecr.7b04246.
 - (17) Perkins, E.; Brown, T.; Berman, R. PT-system, TX-system, PX-system: Three programs which calculate pressure-temperature-composition phase diagrams. *Comp. Geosci.* **1986**, *12*, 749–755, DOI: 10.1016/0098-3004(86)90028-2.
 - (18) Michelsen, M. L.; Møllerup, J. M. *Thermodynamic Models: Fundamentals &*

Computational Aspects; Tie-Line Publications, 2007.

- (19) Venkatarathnam, G. Density Marching Method for Calculating Phase Envelopes. 2. Three-Phase Envelopes. *Ind. Eng. Chem. Res.* **2014**, *53*, 12122–12128, DOI: 10.1021/ie501838y.
- (20) Mokhatab, S. Three-Phase Flash Calculation for Hydrocarbon Systems Containing Water. *Theor. Found. Chem. Eng.* **2003**, *37*, 291–294, DOI: 10.1023/a:1024043924225.
- (21) Connolly, M.; Pan, H.; Tchelepi, H. Three-Phase Equilibrium Computations for Hydrocarbon–Water Mixtures Using a Reduced Variables Method. *Ind. Eng. Chem. Res.* **2019**, *58*, 14954–14974, DOI: 10.1021/acs.iecr.9b00695.
- (22) Jäger, A. Complex Phase Equilibria of Gas Hydrates and other Solid and Fluid Phases Modeled With Highly Accurate Equations of State. Ph.D. thesis, Ruhr-Universität Bochum, 2015.
- (23) Hinojosa-Gómez, H.; Solares-Ramírez, J.; Bazúa-Rueda, E. R. An improved algorithm for the three-fluid-phase VLLE flash calculation. *AIChE J.* **2015**, *61*, 3081–3093, DOI: 10.1002/aic.14946.
- (24) Wu, J.-S.; Bishnoi, P. An algorithm for three-phase equilibrium calculations. *Comput. Chem. Eng.* **1986**, *10*, 269–276, DOI: 10.1016/0098-1354(86)85008-6.
- (25) Cismondi, M.; Michelsen, M. L. Global phase equilibrium calculations: Critical lines, critical end points and liquid-liquid-vapour equilibrium in binary mixtures. *J. Supercrit. Fluids* **2007**, *39*, 287–295, DOI: 10.1016/j.supflu.2006.03.011.
- (26) Cismondi, M.; Michelsen, M. Automated calculation of complete Pxy and Txy diagrams for binary systems. *Fluid Phase Equilib.* **2007**, *259*, 228–234, DOI: 10.1016/j.fluid.2007.07.019.
- (27) Baker, L.; Pierce, A.; Luks, K. Gibbs Energy Analysis of Phase Equilibria. *Soc. Petrol. Eng. J.* **1982**, *22*, 731–742, DOI: 10.2118/9806-pa.
- (28) Michelsen, M. The isothermal flash problem. Part I. Stability. *Fluid Phase Equilib.* **1982**, *9*, 1–19, DOI: 10.1016/0378-3812(82)85001-2.
- (29) Span, R.; Beckmüller, R.; Hielscher, S.; Jäger, A.; Mickoleit, E.; Neumann, T.; Pohl, S.; Semrau, B.; Thol, M. TREND. Thermodynamic Reference and Engineering Data 5.0. 2020; <http://www.thermo.ruhr-uni-bochum.de/>.
- (30) Deiters, U. K.; Bell, I. H. Calculation of Critical Curves of Fluid Mixtures through Solution of Differential Equations. *Ind. Eng. Chem. Res.* **2020**, *59*, 19062–19076, DOI: 10.1021/acs.iecr.0c03667.
- (31) Llave, F. M.; Luks, K. D.; Kohn, J. P. Three-phase liquid-liquid-vapor equilibria in the binary systems nitrogen + ethane and nitrogen + propane. *J. Chem. Eng. Data.* **1985**, *30*, 435–438, DOI: 10.1021/je00042a019.
- (32) Harvey, A. H. What the Thermophysical Property Community Should Know About Temperature Scales. *Int. J. Thermophys.* **2021**, *42*, DOI: 10.1007/s10765-021-02915-9.
- (33) Span, R.; Lemmon, E. W.; Jacobsen, R. T.; Wagner, W.; Yokozeki, A. A Reference Equation of State for the Thermodynamic Properties of Nitrogen for Temperatures from 63.151 to 1000 K and Pressures to 2200 MPa. *J. Phys. Chem. Ref. Data* **2000**, *29*, 1361–1433, DOI: 10.1063/1.1349047.
- (34) Buecker, D.; Wagner, W. A Reference Equation of State for the Thermodynamic Properties of Ethane for Temperatures from the Melting Line to 675 K and Pressures up to 900 MPa. *J. Phys. Chem. Ref. Data* **2006**, *35*, 205–266, DOI: 10.1063/1.1859286.

- (35) Kunz, O.; Klimeck, R.; Wagner, W.; Jaeschke, M. *The GERG-2004 Wide-Range Equation of State for Natural Gases and Other Mixtures*; VDI Verlag GmbH, 2007.
- (36) Lemmon, E. W.; Bell, I. H.; Huber, M. L.; McLinden, M. O. NIST Standard Reference Database 23: Reference Fluid Thermodynamic and Transport Properties-REFPROP, Version 10.0, National Institute of Standards and Technology. <http://www.nist.gov/srd/nist23.cfm>, 2018.
- (37) Bell, I. H.; Wronski, J.; Quoilin, S.; Lemort, V. Pure and Pseudo-pure Fluid Thermophysical Property Evaluation and the Open-Source Thermophysical Property Library CoolProp. *Ind. Eng. Chem. Res.* **2014**, *53*, 2498–2508, DOI: 10.1021/ie4033999.
- (38) Yu, P.; Elshayal, I. M.; Lu, B. C.-Y. Liquid-liquid-vapor equilibria in the nitrogen-methane-ethane system. *Can. J. Chem. Eng.* **1969**, *47*, 495–498, DOI: 10.1002/cjce.5450470516.
- (39) Gasem, K.; Hiza, M.; Kidnay, A. Phase behavior in the nitrogen + ethylene system from 120 to 200 K. *Fluid Phase Equilib.* **1981**, *6*, 181–189, DOI: 10.1016/0378-3812(81)85003-0.